Detecting Deterioration in Electrochemical Sensing Au Electrodes with Admittance Measurement

1st Xin Zhang
Department of Electrical and Electronic Engineering
University College London,London, United Kingdom
xin-zhang@ucl.ac.uk

2nd Sara Ghoreishizadeh
Department of Electrical and Electronic Engineering
University College London, London, United Kingdom
s.ghoreishizadeh@ucl.ac.uk

Abstract—**This paper assesses the impact of deterioration induced by biofouling and halide-mediated passivation (HMP) on the electrochemical impedance and sensing performance of gold screen-printed electrodes (SPEs). Two sets of experiments were carried out in phosphate-buffered saline (PBS) solution which contains chloride ion (to cause HMP) and the same buffer solution enriched with mucin protein (to cause biofouling as well as HMP). The results confirm the existence and role of biofouling and HMP in degrading sensing performance. A decline of more than 50% in sensitivity was set as a threshold for sensor end of lifetime or failure. Concurrent electrochemical impedance spectroscopy labelled with sensor status (healthy, failed) was used to train a decision tree-based classification. A near 100% accuracy was achieved in predicting the sensor health state using only one feature: sensor admittance at a single frequency.**

Index Terms—**biofouling, screen-printed electrodes, halide-mediated passivation, electrochemical impedance spectroscopy, sensor classification, and decision tree.**

I. INTRODUCTION

Electrochemical biosensors are extensively utilized across various applications, including point-of-care diagnostics, environmental monitoring and food safety, owing to their high sensitivity, selectivity, compactness, and cost-effectiveness [1]–[3]. Despite these advantages, halid-mediated and biofouling pose significant challenges to the long-term reliability of electrochemical biosensors [4]–[7] when that are in contact with any fluid that may contain halide ions (e.g. fluoride (F-), chloride (Cl-), iodide (I-)).

Gold is one of the most popular choices for electrode surfaces due to its inertness and biocompatibility. However, when exposed to a solution containing halide ions, the gold surface is firstly etched by the halide ions with the formation of a soluble halide-gold complex [8]. Subsequently, a portion of the dissolved gold ions is re-deposited onto the electrode surface [9]–[11], initiating a heterogeneous reaction and ultimately culminating in the establishment of a passive surface layer on the electrodes [11], called halid-mediated passivation (HMP). This affects the structural integrity and decreases the reproducibility of the electrode surface.

On the other hand, biofouling denotes the adsorption of cells, proteins, peptides, lipids and other biological materials onto the surface of an electrode in contact with biological fluid or other tissues [6], [7]. Biofouling obstructs the surfaces of electrodes thereby limiting the area available for charge transfer between the electrode and electrolyte, an essential transduction mechanism in amperometric sensors. To mitigate the interference caused by biofouling, strategies such as the pre-treatment of samples, anti-biofouling modifications and the utilization of disposable biosensors have been adopted [12]. However these methods may not be suitable in scenarios where long-term monitoring is required (e.g. wearable and implantable applications); Sensor replacement may not be possible depending on the location of the device in/on the body, pre-treating the sample may lead to higher overall sensor production that make the technology unattractive for low resource settings [13], [14], and anti-biofouling coatings typically reduce sensor's sensitivity [15].

An alternative technique is to instead work with an "array" of sensing electrodes. This not only provides redundancy, in case a sensor fails due to HMP or biofouling but also enables parallel and simultaneous measurement of same (or multiple) analytes that can improve the reliability of measurements. An essential function that is required in such a system is to determine which sensors within the array have failed (e.g. due to biofouling or HMP) so they can be replaced with other sensors within the array or their weight in overall measurement be reduced or cancelled altogether.

Electrochemical impedance spectroscopy (EIS) has been previously used to evaluate the health condition of various systems, including lithium-ion battery cells [16], membrane filtration system [17] and glucose sensor [18]. In particular, it has been reported that some parameters extracted from EIS, such as charge transfer resistance (R_{ct}) and double layer capacitance (C_{dl}), exhibit a strong correlation with the sensor's sensitivity [3], [18]. However, deriving such parameters requires running a full electrochemical impedance measurement at several frequencies followed by curve fitting algorithms to estimate the parameters from the raw EIS data. Producing sine waves at several frequencies is an energy and resource-consuming task, and curve fitting algorithms are computationally complex, making such a solution unsuitable for point-of-care or low-resource settings with limited hardware capabilities and large sensor arrays.

In this work, we present a lightweight method to determine the state of health of the sensors that are experimentally driven from parallel EIS and sensitivity measurement on a large number of commercially available gold screen printed elec-
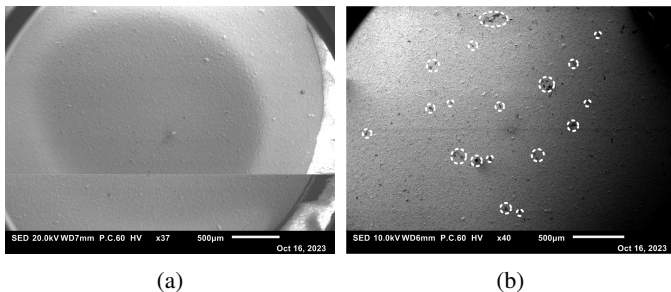
Fig. 1: SEM images of (a) a fresh Au-SPE (b) same Au-SPE after 6-hrs incubation in mucin solution with the circle highlighting the adsorbed mucin.

trodes (SPEs). The electrodes were frequency-characterised when undergoing accelerated biofouling and HMP. A feature engineering was then carried out to find the smallest set of features that not only achieve high accuracy classification but can be implemented using minimal hardware and resources.

II. ELECTROCHEMICAL CHARACTERISATION DURING INCUBATION: MATERIALS AND METHODS

A. Electrodes, chemicals, and equipment

Gold SPEs (C220AT) with a working electrode diameter of $4mm$ purchased from DropSens. A short thin rod of a platinum electrode and an Ag/AgCl electrode was utilized as counter electrode and reference electrode respectively. PBS tablet, mucin from the porcine stomach, potassium ferricyanide(III) and potassium hexacyanoferrate(II) trihydrate were purchased from Sigma-Aldrich. De-ionised water (DI) was prepared with the Milli-Q system. The buffer solution was prepared by dissolving one PBS tablet into 200 ml DI. Mucin solution was prepared by dissolving 270 mg mucin protein into 10 ml of PBS solution. 5 mM and 2.5 mM potassium ferri/ferrocyanide solutions were prepared by dissolving 82.31 mg of potassium ferricyanide and 105.6 mg of potassium hexacyanoferrate(II) trihydrate into 50 ml and 100 ml of PBS solution respectively. All solutions were stored at 4 °C while not used. EIS and CV measurements were performed with Autolab PGSTAT204 from Metrohm. Scanning Electron Microscopy(SEM) was carried out using JEOL JSM IT-100 SEM machine.

B. Experiment design

To distinguish any differences between EIS due to HMP and biofouling, SPEs were studied in two groups. Group A was designed to assess the impact of HMP where SPEs were kept in PBS buffer for several days. In Group B, electrodes were instead kept in a mucin-enriched PBS solution, that would cause biofouling in addition to HMP. A total of 28 electrodes were used, that is 14 electrodes in each group.

In both groups, the temperature was controlled throughout the entire time by keeping the electrodes (and solutions) in an incubator at 37 °C. To accelerate biofouling, a high concentration of mucin, 27 mg/ml that is roughly 10 times its salivary levels was used. Frequent EIS and cyclic voltammetry

(CV) measurements were carried out on four electrodes at specific time points within 3 days after starting the incubation.

C. EIS and sensitivity measurements

The frequency range of EIS measurements was from 0.1 Hz to 1 MHz with an amplitude of 5 mV. This yielded the complex impedance at 141 specific frequencies, within the above frequency range.

To gauge the sensing performance of the electrodes, CV measurements were conducted in 5 mM and 2.5 mM potassium ferri/ferro-cyanide solutions sequentially, with potential sweeping from -0.4 V to 0.6 V at a scan rate of 100 mV/s. The sensing performance, hereafter referred to as "sensitivity" for simplicity, was defined as the difference between the peak current (at 173.8 mV) at 5 mM and 2.5 mM potassium ferri/ferro-cyanide concentrations, divided by the concentration difference (2.5 mM).

After initial characterisation of each SPE with EIS and CV, they were all rinsed with DI water and incubated.Sequential EIS and CV measurements were then carried out at seven specific time points from the start of incubation: 30 minutes, 1 hour, 6 hours, 12 hours, 1 day, 2 days, and 3 days. At this point day, all electrodes showed lower than 50% sensitivity.

At each time point, two SPEs from group A and two from group B were taken out of the incubator, rinsed with DI water and underwent EIS and then sensitivity measurement one at a time. These four electrodes were then discarded and did not continue to incubation, because CV measurement itself is expected to change the surface of the electrodes [19]. Overall, 56 measurements were carried out, two per SPE (one before and one after the start of incubation).

III. ELECTROCHEMICAL CHARACTERISATION DURING INCUBATION: RESULTS AND DISCUSSION

The existence of biofouling induced by the proposed recipe is confirmed by comparing the SEM images of a new SPE (Figure 1(a)) and the same SPE after 6 hours of incubation in mucin enriched buffer solution (Figure 1(b)). The adsorption of mucin proteins form visually discernible structures that can be observed by SEM as dark areas in Fig. 1(b).

The measured average sensitivity of 28 fresh SPEs was 40.6±6.1 $\mu A/mM$ prior to the incubation. Therefore, the threshold of the fault was set for 20.3 $\mu A/mM$ (dashed lines in Fig. 2). The long-term sensitivity measurement results are presented in Fig. 2(a). It can be observed that in both groups the sensitivity decreases with incubation time, while the change of sensitivities of Group B, is more significant than that of Group A. This was expected as SPEs in group A only undergo HMP while group B undergo both biofouling and HMP.

In figure 2(b) and (c), two series of Nyquist plots of each group are shown. The diameters of the semi-circles, which serve as indicators of the charge transfer resistance of the sensors, exhibit an increasing trend in each group over the incubation time. Fitting the EIS data to the randles equivalent model of the sensor was used to extract R_{ct} values. These are
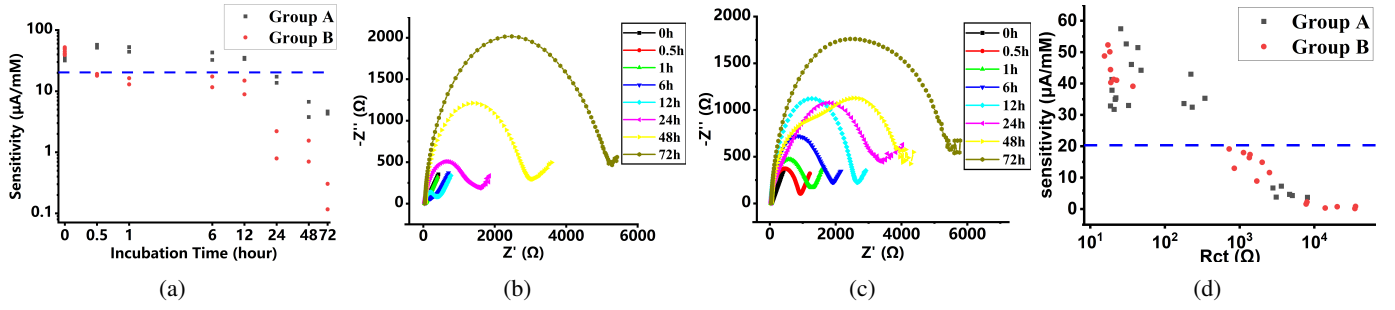
Fig. 2: (a) plot the sensitivity aginst the incubation time of Group A and Group B with a dash line indicating the threshold of fault. (b) Nyquist plots measures on sensors before incubation and after 0.5 hours to 72 hours of Group A. (c) Nyquist plots measures on sensors before incubation and after 0.5 hours to 72 hours of Group B. (d) plot the sensitivities against the correspond R_{ct}, with a dash line indicating the threshold of fault.
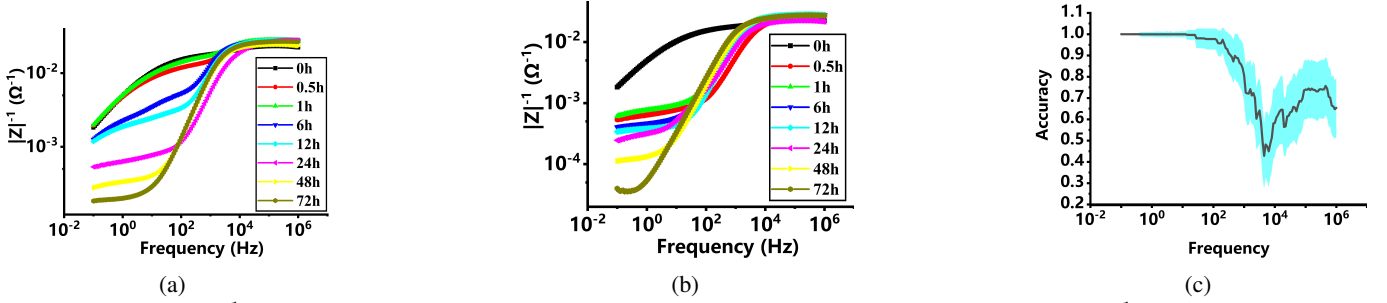

Fig. 3: (a) plots of $\frac{1}{|Z|}$ against frequency of SPEs of Group A after 0 hour to 72 hours. (b) plots of $\frac{1}{|Z|}$ against frequency of SPEs of Group A after 0 hour to 72 hours. (c) plot the prediction accuracy against the specific frequency selected as the only feature of the decision tree, with the error bar showed in shaded area.

plotted versus SPE sensitivity in Fig 2(d). Two clusters can be visually distinguished above and below the threshold line. This is consistent with findings previously reported [3], [18].

In search of a more easily measurable feature, the admittance, $\frac{1}{|Z|}$ of the SPE was considered in this work. The admittance is plotted versus frequency and time in Fig. 3(a) and 3(b) for sensors in Groups A and B. A visual assessment indicates areas where the admittance of substantial changes exists at low-frequency ranges.

IV. FEATURE SELECTION AND CLASSIFIER DESIGN

The correlation between the admittance and sensitivity is obvious in the low-frequency ranges as shown in Fig. 3(a) and (b), suggesting the possibility of manual classification of SPEs. However, to allow scalability of the classification and its robustness, a machine learning feature selection and classification technique was adopted in this work. As previously stated, a total of 141 frequencies were used in EIS measurement, leading to 141 measured $\frac{1}{|Z|}$. The importance of each one of these values in the accurate prediction of the SPE health state was evaluated using a random forest model. To train the random forest model, the dataset containing all 141 $\frac{1}{|Z|}$ values was fed to the model as the features and the labels (failed, healthy) obtained through concurrent sensitivity measurement were used as outputs. A decision-tree-based machine learning classifier was then trained with the selected feature subset, starting from 10 most important frequencies, then to only the single most important feature. To develop the classifier, the

dataset including 56 measurements is divided into 80% of training (44 data) and 20% testing samples(12 data). Data were randomized to ensure robustness, with accuracy assessments conducted across all 558.383 billions of combinations to determine the model's reliability. The achieved average accuracy and its variation at each specific frequency is plotted in Fig. 3 (c). The highest accuracy achieved among all frequencies is 99.98%, with any one of frequencies from $0.1Hz$ to $12.589Hz$. The lower frequencies achieve a high prediction accuracy with a low error bar which means the admittance at these frequencies is suitable for use as a single feature in classifying the SPE sensor.

V. CONCLUSION

The feature extraction and selection method enable the machine learning classifier to achieve a near 100% accuracy on detecting a failed SPE caused by either biofouling or HMP with only one feature: admittance at any single frequency from $0.1Hz$ to $12.589Hz$. This admittance feature is more efficient than conventional R_{ct} or C_{dl} measurements in terms of time and energy. This work will be further advanced by considering the impact of other deterioration sources and environmental factors such as temperature and pH, which are limitations of current work. Future works include validating the classifier on gold microelectrodes prior to developing an embedded and compact circuit for in-situ fault detection in microelectrode sensor arrays.

REFERENCES

[1] M. Li, A. A. S. Gill, A. Vanhoestenberghe, and S. S. Ghoreishizadeh, "An integrated circuit for galvanostatic electrodeposition of on-chip electrochemical sensors," in *2022 29th IEEE International Conference on Electronics, Circuits and Systems (ICECS)*, 2022, pp. 1–4.

[2] A. J. Bandodkar and J. Wang, "Non-invasive wearable electrochemical sensors: a review," *Trends in biotechnology.*, vol. 32, no. 7, pp. 363–371, 2014.

[3] S. S. Ghoreishizadeh, X. Zhang, S. Sharma, and P. Georgiou, "Study of electrochemical impedance of a continuous glucose monitoring sensor and its correlation with sensor performance," *IEEE sensors letters.*, vol. 2, no. 1, 2018.

[4] N. Wisniewski and M. Reichert, "Methods for reducing biosensor membrane biofouling," *Colloids and surfaces.*, vol. 18, no. 3-4, pp. 197–219, 2000.

[5] J. Kuhlmann, L. Dzugan, and W. Heineman, "Comparison of the effects of biofouling on voltammetric and potentiometric measurements," *Electroanalysis*, vol. 24, no. 8, pp. 1732–1738, 2012.

[6] N. Wisniewski, F. Moussy, and W. Reichert, "Characterization of implantable biosensor membrane biofouling," *Fresenius' journal of analytical chemistry*, vol. 366, no. 6-7, pp. 611–621, 2000.

[7] M. KYROLAINEN, P. RIGSBY, S. EDDY, and P. VADGAMA, "Biocompatibility hemocompatibility - implications and outcomes for sensors," *Acta anaesthesiologica Scandinavica.*, vol. 39, pp. 55–60, 1995.

[8] A. J. Bard, L. R. Faulkner, and H. S. White, *Electrochemical methods: fundamentals and applications.* John Wiley & Sons, 2022.

[9] O. Kasian, N. Kulyk, A. Mingers, A. R. Zeradjanin, K. J. J. Mayrhofer, S. Cherevko, O. Kasian, N. Kulyk, A. Mingers, A. R. Zeradjanin, K. J. Mayrhofer, and S. Cherevko, "Electrochemical dissolution of gold in presence of chloride and bromide traces studied by on-line electrochemical inductively coupled plasma mass spectrometry," *Electrochimica acta*, vol. 222, pp. 1056–1063, 2016-12.

[10] J. Ribeiro, E. Silva, and C. Pereira, "Electrochemical characterization of redox probes at gold screen-printed electrodes: Efforts towards signal stability," *ChemistrySelect.*, vol. 5, no. 17, pp. 5041–5048, 2020.

[11] X. Xu, A. Makaraviciute, and Z. Zhang, "Revisiting the factors influencing gold electrodes prepared using cyclic voltammetry," *Sensors and actuators.*, vol. 283, pp. 146–153, 2019.

[12] L. Zhou, X. Li, B. Zhu, and B. Su, "An overview of antifouling strategies for electrochemical analysis," *Electroanalysis*, vol. 34, no. 6, pp. 966–975, 2022.

[13] T. Xiao, F. Wu, J. Hao, M. Zhang, P. Yu, and L. Mao, "In vivo analysis with electrochemical sensors and biosensors," *Analytical Chemistry*, vol. 89, no. 1, pp. 300–313, 2017.

[14] M. Zhang, P. Yu, and L. Mao, "Rational design of surface/interface chemistry for quantitative in vivo monitoring of brain chemistry," *Accounts of Chemical Research*, vol. 45, no. 4, pp. 533–543, 2012.

[15] P.-H. Lin and B.-R. Li, "Antifouling strategies in advanced electrochemical sensors and biosensors," *The analyst online /*, vol. 145, no. 4, pp. 1110–1120, 2020.

[16] D. I. Stroe, M. Swierczynski, A. I. Stan, V. Knap, R. Teodorescu, and S. J. Andreasen, "Diagnosis of lithium-ion batteries state-of-health based on electrochemical impedance spectroscopy technique," in *IEEE Energy Conversion Congress and Exposition*, ser. IEEE Energy Conversion Congress and Exposition, IEEE. NEW YORK: IEEE, 2014, pp. 4576–4582.

[17] N. Zhang, H.-J. Lee, Y. Wu, M. A. Ganzoury, and C.-F. de Lannoy, "Integrating biofouling sensing with fouling mitigation in a two-electrode electrically conductive membrane filtration system," *Separation and purification technology*, vol. 288, 2022.

[18] H. Sharma, D. Kalita, and K. Mirza, "Prediction of glucose sensor sensitivity in the presence of biofouling using machine learning and electrochemical impedance spectroscopy," *IEEE sensors journal.*, vol. 23, no. 16, pp. 18 785–18 797, 2023.

[19] X. Hua, H.-L. Xia, and Y.-T. Long, "Revisiting a classical redox process on a gold electrode by operando tof-sims: where does the gold go?" *Chemical science.*, vol. 10, no. 24, pp. 6215–6219, 2019.